Tutor/es
Sra. Núria López Vinent
Dr. Jaume Giménez Farreras
Departament d'Enginyeria Química i Química Analítica

Grau en Enginyeria Química

Treball Final de Grau

Matrix influence on the treatment of emerging pollutants by advanced oxidation processes.

Coral Gutiérrez Fernández

June 2018

UNIVERSITAT DE BARCELONA

Tot el que va arribar on està, va haver de començar on era.

Robert Louis Stevenson

En primer lloc, agrair a la meva família per haver-me ensenyat a ser persistent i constant a l'hora d'assolir els meus objectius en la vida.

Gràcies a la Núria López i al Dr. Jaume Giménez per la dedicació, els coneixements i l'ajuda aportada al llarg d'aquest projecte.

Finalment agrair als amics els qui, dia rere dia, han fet d'aquest camí un camí més amè i agradable.

A tots vosaltres, moltes gràcies.

CONTENTS

SUMMARY

The shortage of fresh water in the world is a growing problem that, added to the high anthropogenic contamination of this resource, makes the advance in new technologies and developments of water recovery a priority need.

Advanced oxidation processes (AOPs) can be an useful technique for the wastewaters treatment. Some AOPs need light and have used lamps of low or medium pressure as a source of UV radiation. The short life-time, high energy consumption and the presence of mercury in its components make it necessary to think of an alternative for these conventional lamps. Nowadays, studies have been carried out that suggest the source of LED light as a viable alternative, owing to LEDs have a low energy consumption, a long life-time and are mercury free. Besides the efficiency of the results of the oxidation of emerging pollutants through the photo-Fenton process, this process is used in this study but with LEDs (λ = 365-370 nm) for the treatment of the propranolol drug.

On the other hand, an important aspect in the AOPs is the influence of the water matrix because it can significantly interfere with the process. For this reason, this project has experienced with four effluent waters from the secondary treatments from two different WWTPs. The treatments are: secondary with nutrient elimination, without elimination of nutrients, Integrated Fixed-film Activated Sludge (IFAS) and Membrane Bioreactor (MBR). However, ultrapure water has also been tested to make comparisons with the other matrices.

All experiments have been carried out by setting a 2L batch reactor, 8W total power lamp and pH of 2.8. The ratio in ppm of Fe(II)/H_2O_2 used was 0.07 and the concentration of propranolol 50 ppm.

Finally, it has been shown that with the Milli-Q water matrix, a 100% degradation is obtained at the end of the experiment in both BLB and LED. Regarding the WWTP matrices, the propranolol highest degradation corresponds to MBR with a result of 95.28% in BLB and AEN with 52.91% in

LED. In contrast, IFAS showed degradations of 70.25% and 32.91% in BLB and LED respectively, being the matrix with the lowest degradation of the pollutant.

Keywords: Propranolol, Advanced Oxidation Processes, Efficiency, Photo-Fenton, UV-LED, BLB.

RESUM

L'escassetat d'aigua dolça en el món és un problema creixent que, sumat a l'elevada contaminació per causes antropogèniques d'aquest recurs, fa que hi hagi una necessitat prioritària en l'avenç i desenvolupament de noves tecnologies de recuperació de l'aigua.

Els processos d'oxidació avançada (POAs) poden ser una alternativa en el tractament d'aigües. Alguns POAs utilitzen llum UV i, tradicionalment, s'han fet servir làmpades de baixa o mitja pressió com a font de radiació UV. Un temps útil de vida curt, un alt consum energètic i la presencia de mercuri en els seus components fan que s'hagi de pensar en una alternativa per a aquestes làmpades convencionals. En l'actualitat s'han realitzat estudis que plantegen el LED, com una alternativa viable, ja que aquesta font de radiació presenta un baix consum energètic, un llarg temps de vida útil i està lliure de mercuri. Degut a l'eficiència dels resultats de l'oxidació de contaminants emergents mitjançant el procés de foto-Fenton, en aquest estudi es fa servir aquest procés però amb LEDs (λ=365-370 nm) per al tractament del fàrmac propranolol.

D'altre banda un aspecte important en els (POAs) es la influència de la matriu aquosa, ja que aquesta pot interferir notablement en el procés. Per aquesta raó en aquest projecte s'ha experimentat amb quatre aigües procedents d'efluents provinents de quatre tractaments secundaris de dos EDAR diferents. Els tractaments són: secundari amb eliminació de nutrients, sense eliminació de nutrients, Inegrated Fixed-film Activated Sludge (IFAS) i Bioreactor de Membrana (MBR). Tanmateix també s'ha assajat com a matriu l'aigua ultrapura a fi d'establir comparacions amb les altres matrius.

Tots els experiments s'han realitzat amb un reactor discontinu de 2L, una làmpada de 8W de potencia (LED o BLB) i un pH de treball de 2,8. La ràtio en ppm de $Fe(II)/H_2O_2$ utilitzada va ser de 0.07 i la concentració inicial de propranolol 50 ppm.

Finalment s'ha obtingut que amb la matriu d'aigua Milli-Q s'obté una degradació del 100% al finalitzar l'experiment tant en BLB com en LED. Pel que respecta a les matrius d'EDAR, la degradació del propranolol major es correspon a MBR amb un resultat del 95,28% en BLB i AEN

amb un 52,91 en LED. En contraposició IFAS ha presentat un 70,25% i un 32,91% en BLB i LED respectivament, sent la matriu amb menor degradació del contaminant.

Paraules clau: Propranolol, Processos d'Oxidació Avançada, Eficiència, Foto-Fenton, UV-LED, BLB.

1. INTRODUCTION

Water is a necessary benefit for the human being and the planet's ecosystem. This is due to the fact that all life forms need water as an essential element and that is why it becomes a resource of high value that must be conserved.

Currently, it can be considered that the lack of fresh water is a real problem because the available sources of fresh water are being depleted. The excessive growth of the population, the improvement of the quality of life and the industrialization have caused a great need for fresh water. This need is difficult to satisfy owing to the climatic conditions of recent years have caused drought situations in many regions.[1] Spain is at present considered the driest country in Europe. This fact activates the alarm in view to change this unfavourable situation.[2] Also, according to the 2018 United Nations report, 3.6 billion people (nearly half the global population) live in areas that are potentially water-scarce at least one month per year, and this population could increase to 4.8–5.7 billion by 2050.[3]

Water is considered contaminated when it has been used for any human activity and loses the minimum quality to be used again directly. The origin of aquatic pollution falls on anthropogenic activities and is mainly produced by industrialization, agriculture and urban waste. Water is also a vital element used by humans in their routine activities like alimentation, cleaning tasks and personal care, this is what encourage new and improved technologies about recovery and reuse of fresh water.

1.1. EMERGENT POLLUTANTS

Nowadays, pollutants derived from cleaning products, cosmetics, personal hygiene and pharmaceutical compounds arrive to water treatment plants (WWTPs) every day and these contaminants could not be eliminated by conventional biological methods because their biodegradability is too low. These pollutants are called emerging contaminants (ECs) and they

are found in slight concentrations (ppm or ppb). However, the presence of this pollutants is a hazard both to environment and humans because many of these contaminants can transform in the environment, from such processes as microbial degradation, photolysis, and hydrolysis, and they can also react with disinfectants in drinking water or wastewater treatment to form disinfection by-products. Issues surrounding these emerging contaminants include bioaccumulation, persistence, and toxicity.[4,5]

1.2. **PROPRANOLOL**

Propranolol (PROP) is a type of nonselective drug called beta-blocker.[6] It works by acting on the nerve impulses in specific areas of the body such as the heart. It was the first success beta-blocker made and the one which active principle was demonstrated with prophylaxis and migraine headaches.

This drug was developed in the 1960s by the scientist James W. Black. It was obtained by modification of pronethalol and dichloroisoprenaline. The key difference, which was carried through to essentially all subsequent beta blockers, was the inclusion of an oxymethylene group (-O-CH2-) between the aryl and ethanolamine moieties of pronethalol, greatly increasing the power of the compound.

PROP is widely used for the therapy of hypertension[7], cardiac arrhythmias, angina pectoris, hyperthyroidism and infantile hemangiomas.[8] Also, is used to attenuate physical manifestations of anxiety such as tremors, tachycardia, palpitations, sweating etc.

This pharmaceutical compound is generally administered orally by conventional tablets notwithstanding the above it could be administered by intravenous injection. After PROP administration the dose is almost completely absorbed reaching peak concentrations in 60-90 minutes. The drug is mainly eliminated by the kidneys although it is also eliminated by excretion having the elimination half-life of PROP ranges from 2 to 6 hours.[9]

Chemical structure of PROP (Figure 1) shows the presence of chiral centre where it happens the binding to the receiver for perform its biological action.[10]

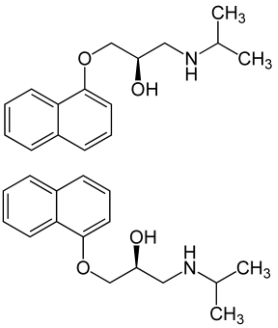

Figure 1. Structural formulate of PROP enantiomers. Source: ChemDraw.

1.3. **LEGAL FRAMEWORK**

The Water Framework Directive (WFD) of the EU, adopted in the year 2008, has a pioneering approach to water protection, based in natural geographic formations; particularly the watersheds. The WFD arises from the need to unify all the water management areas in Europe and here are some of its bases:

- Prevent water deterioration.
- Improve and restore the state of surface water bodies.
- Ensure that surface water is in good chemical and ecological condition.
- Reduce pollution due to discharges and emissions of hazardous substances.
- Protect, improve and restore groundwater, prevent its contamination and deterioration and guarantee a balance between its collection and renewal.

This directive involves the identification of priority substances among those that represent a significant risk to the aquatic environment through the Union or through it. Then, in Decision 2455/2001/EC of the European Parliament and of the Council of 20 November 2001, establishing the list of priority substances in the field of water policy, the list had 33 substances or groups of substances.[11,12]

This directive has been updated in the current Directive 2013/39/EU of the European Parliament and of the Council of 12 August 2013 that promotes the preventive action and the polluter pays principle, the identification of pollution causes, dealing with emissions of pollutants

at the source, and finally the development of innovative water/wastewater treatment technologies, avoiding expensive solutions.

According to the Directive 2013/39/EU "A new mechanism is needed to provide the Commission with targeted high-quality monitoring information on the concentration of substances in the aquatic environment, with a focus on emerging pollutants and substances for which available monitoring data are of insufficient quality for risk assessment." [13]

1.4. ADVANCED OXIDATION PROCESSES (AOPS)

The so-called ECs must be removed from waste water at the WWTPs because as it has previously been shown, they are potentially dangerous for both environment and health[14]. The way for this degradation is do it with advanced oxidation processes (AOPs) which are called to fill the gap between the treatability attained by conventional physico-chemical and biological treatments and the day-to-day more exigent limits fixed by environmental regulations.[15]

These treatments are based on chemical processes capable of producing large changes in the chemical structure of pollutants, involving the generation and use of powerful oxidizing species, mainly the hydroxyl radical (HO·). This radical has a high oxidative capacity (E_0 2.80V) and can easily break molecule bonds. It is an oxidizing species with low selectivity, very short life and has also a great reactivity with almost every type of organic substances, degrading it to less complex compounds. [16,17,18]

AOPs can be classified in photochemical processes or non-photochemical processes If radiation has a participation in the processes or not respectively.

Table 1. AOPs photochemical classification. (Litter & Quici, 2010) [19]

AOP	Type
O_3/UV	
H_2O_2/UV	
O_3/ H_2O_2/UV	
Photo-Fenton	Photochemical
TiO_2/UV	
Photolysis	
TiO_2/H_2O_2/UV	

Ozonation at alkaline pH (>8,5)	
Ozone + catalyst	
Fenton	Non-photochemical
Ultrasonic cavitation	
Non-thermal plasma	

1.4.1. Fenton

This AOP bears the name of its discoverer, Henry J. Fenton, and it consists of a series of reactions shown below:

$Fe\ (II) + H_2O_2 \longrightarrow Fe(III) + OH^- + HO^{\bullet}$ Eq. 1.1

$Fe\ (III) + H_2O_2 \longrightarrow Fe(II) + HO_2^{\bullet} + H^+$ Eq. 1.2

$HO + H_2O_2 \longrightarrow HO_2^{\bullet} + H_2O$ Eq. 1.3

$HO^{\cdot} + Fe\ (II) \longrightarrow Fe\ (III) + OH^-$ Eq. 1.4

$Fe\ (III) + HO_2^{\bullet} \longrightarrow Fe\ (II) + O_2 + H^+$ Eq. 1.5

$Fe\ (II) + HO_2^{\bullet} + H^+ \longrightarrow Fe\ (III) + H_2O_2$ Eq. 1.6

$HO_2^{\bullet} + HO_2^{\bullet} \longrightarrow H_2O_2 + O_2$ Eq. 1.7

As we can see iron cation stands on a cycle between both oxidation states II and III. As far as the hydroxyl radical is concerned it is created at Eq.1.1, from that moment takes place the oxidation of organic compounds and the formation of Fe(III) too. It is important do the reactions at pH close to 3 because in this condition the $[Fe(H_2O)_5(OH)]^+$ complex becomes the predominant stable specie and it is the catalysts of reaction. On one hand if we work at pH lower than 3 we have the predomination of Fe(III) ion and it is not convenient for the kinetic of the reaction. On the other hand, if pH rises upper than 3, precipitates of iron appear ($Fe(OH)_2^+$ and $Fe_2(OH)_2^{4+}$).[20,21,22]

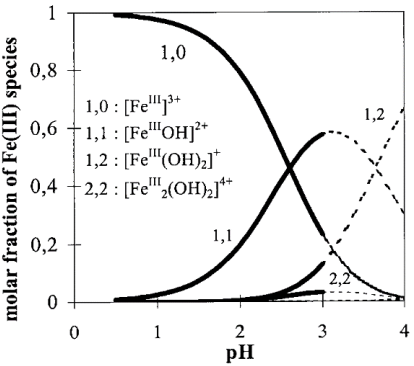

Figure 2. Speciation of Fe(III) species in acidic aqueous solution. Source: H. Gallard et al, 1999.

Fenton is one of the most studied AOPs, due to its efficiency, low reaction time, and easy application. (Pignatello et al., 2006)

1.4.2. Photo-Fenton

This AOP is based on principles that are common to Fenton making use of a catalyst like Fe (II) ion but with simultaneous use of ultraviolet/visible radiation. Therefore, the photo-Fenton process is faster than dark Fenton and also allows the generation of HO· through three mechanisms: first the decomposition of hydrogen peroxide with the Fe(II) catalyst (Eq.2.1), then the incidence of radiation makes the hydrogen peroxide decomposition into hydroxyl radicals (Eq.2.2) this decomposition is done at wavelengths corresponding to UV-Vis spectrum, and third additional production of HO· radicals upon Fe(II) regeneration (either by Eq.2.3 and Eq.2.4) its promoted using radiation with wavelengths in the range 290<λ<410 nm. Finally, the Fe(II) regeneration is shown at Eq.2.5 (where R= organic compound).[23]

$$Fe\ (II) + H_2O_2 \rightarrow Fe\ (III) + OH^- + HO^{\cdot} \qquad \text{Eq. 2.1}$$

$$H_2O_2 + h\nu \rightarrow 2HO^{\cdot} \qquad \text{Eq. 2.2}$$

$$Fe\ (III) + H_2O_2 + h\nu \rightarrow Fe\ (II) + HO^{\cdot} + H^+ \qquad \text{Eq. 2.3}$$

$$Fe(OH)^2 + h\nu \rightarrow Fe\ (II) + HO^{\cdot} \qquad \text{Eq. 2.4}$$

$$[Fe(RCO_2)]^{2+} + h\nu \rightarrow Fe\ (II) + CO_2 + R^{\cdot} \qquad \text{Eq. 2.5}$$

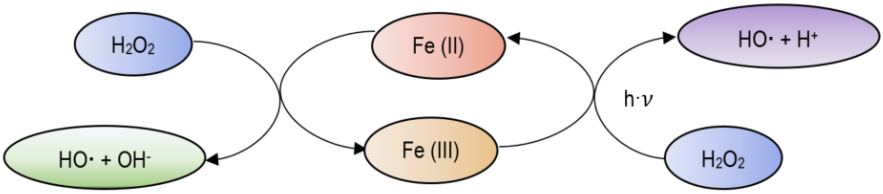

Figure 3. Photo-Fenton cycle schema.

2. JUSTIFICATION

2.1. EMERGENT CONTAMINANT AND AOP SELECTION

Over the last ten years the study about the AOPs and the ECs have been increased exponentially (Figure 4). According to the Association of British Pharmaceutical Industry (ABPI) in the report titled "International Comparison of Medicines Usage: Quantitative Analysis", Spain was ranked as second world largest consumer of pharmaceuticals in 2013. Moreover, beta-blockers have been reported to be found ubiquitously in influents and effluents of WWTPs at trace levels ranging from a few ppb to several hundred ppm (Tran and Gin, 2017). Focusing on PROP, it has been found that this EC appears as effluent in WWTPs of Europe with concentrations of 615 ng/L. For all these reasons PROP has been the emergent contaminant selected to do this project. [24]

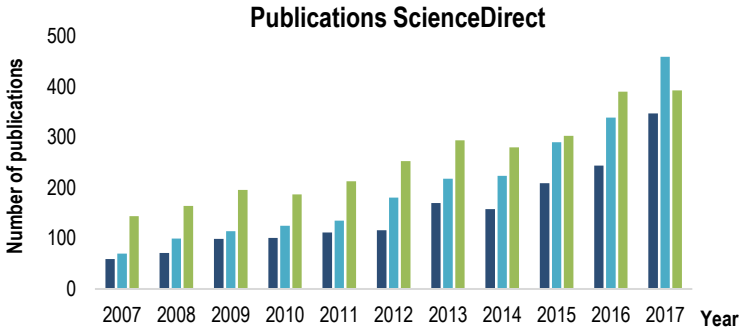

Figure 4. The increase of publications related to ECs, photo-Fenton UV-Visible and photo-Fenton UV-LEDs in the last 10 years. Database: ScienceDirect (Accessed March 16, 2018).

In the previous graph (Figure 4) it is reflected that the processes of advanced oxidation, more specifically photo-Fenton, and emerging contaminants are a subject of notable interest.

2.2. **MATRIX SELECTION**

The project's experiments were carried out using, on the one hand, ultra-pure Milli-Q water matrix and, on the other hand, real water matrices which came from different secondary treatments from two different WWTPs. These matrices were selected to be able to bring the experiments closer to the reality of the water treatment plants. The main reason of the secondary effluents selection is the viability of this process as a tertiary treatment.

2.3. **LIGHT SOURCE SELECTION**

The work seeks to compare the black light blue lamps (BLB) reactor with the ultraviolet light-emitting diode (UV-LED) reactor. At present UV-LED photo-Fenton alternative to BLB is being considered for the elimination of ECs, one of the main reasons is the mercury issue. Mercury lamps are typical radiation sources in UV-induced AOPs and as it is known mercury is a hazard to human health, thus it must be removed of the industrial processes. This is reflected on Minamata Convention on Mercury, which was adopted in 2013, which aimed at providing the gradual phase out of mercury use in several products and processes by 2020.[25] Moreover another of the main reasons for the comparison between both reactors, is the energetic efficiency, which is an important factor to the process economy.[26]

The BLB lamps have the following drawbacks:

- Presents mercury as lamp component.
- Short life-time (above 8,000 h).
- High energy consumption due to their power requirement.
- Overheating and inefficiency.
- Low photonic efficiency.

The expectations point to the UV-Led reactor to be the best way of procedure basically because have the following advantages that are opposed to the BLB reactor:

- It is mercury free.
- Triplicates the life time (until 26,000 h).
- Low power consumption.
- No warming-up time.
- High photonic efficiency. [27,28]

3. OBJECTIVES

The two objectives of this project are, on the one hand, to evaluate the influence of the different real water matrices from two WWTPs and on the other hand to determine the influence of the light source on the degradation of PROP by the photo-Fenton process at acid pH.

As a final point, energetic consideration will carry out comparing the efficiency of the light sources (BLB and UVA-LED) employed in the photo-Fenton process.

4. MATERIALS AND METHODS

4.1. REAGENTS

4.1.1. Pollutant reagent

Propranolol hydrochloride which brand is Sigma-Aldrich Chemical Co.

Table 2. Propranolol hydrochloride properties.[29]

Propriety	Value
Molecular formula	$C_{16}H_{12}NO_2 \cdot HCl$
Molecular structure	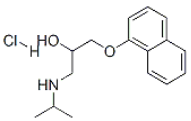
Molecular weight (g/mole)	295.807
CAS No.[30]	318-98-9
Melting Point (ºC)	163-164
Solubility (µg/mL)	>44.4
pKa	9.45
log Kow	-0.45 (pH 2.0)

Absorption spectrum (PROP 50 ppm in Milli-Q water)

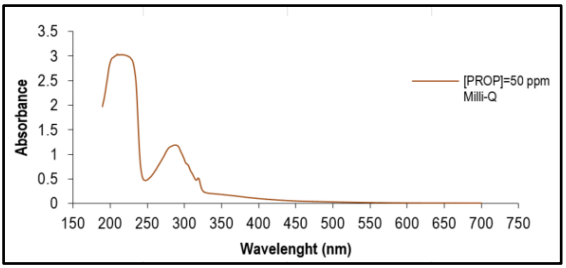

4.1.2. Other chemicals reagents

The following table shows the other reagents used in the experiments:

Table 3. Information about reagents. [29]

Name	CAS No.	Formula	Company	Purity (%)	Used in/for
Acetonitrile	75-05-8	CH_3CN	Fischer Chemical	99.80	HPLC analysis
Ammonium metavanadate	7803-55-6	H_4NO_3V	Sigma Aldrich	99	H_2O_2 determination
Ascorbic acid	50-81-7	$C_6H_8O_6$	Panreac Química	91	Totally Fe determination
Hydrogen peroxide	7722-84-1	H_2O_2	Merck	30 w/w	Photo-Fenton
Iron (II) sulphate heptahydrate	7782-63-0	$H_{14}FeO_{11}S$	Panreac Química	30	Photo-Fenton
Liver bovine catalase	9001-05-2	$C_9H_{10}O_3$	Sigma Aldrich	-	To avoid further reactions
Methanol	65-56-1	CH_3OH	Panreac Química	99.90	Stop the reaction with H_2O_2 to HPLC
Orthophosphoric acid	7664-38-2	H_3PO_4	Panreac Química	85	HPLC analysis
Sodium bisulphite	7631-90-5	$NaHSO_3$	Panreac Química	40	Stop the reaction with peroxide to TOC
Sulphuric acid	7664-93-998	H_2SO_4	Panreac Química	98	For pH adjustment

1,10-phenanthroline	66-71-7	$C_{12}H_8N_2$	Sigma Aldrich	99	Fe^{2+} determination

4.2. **WATER MATRIX**

4.2.1. Milli-Q water

Milli-Q water is the name of the ultrapure water. According to international standards as the International Organization for Standardization (ISO) or the American Society for Testing and Materials (ASTM) it is considered ultrapure water when it has been purified by stringent specifications achieving the values 18.2 MΩ·cm of resistivity. These organizations also had their own ultrapure water classification depending water parameters. The name Milli-Q comes from the creator brand Millipore Corporation. [31]

Table 4. Milli-Q matrix properties.

pH	Resistivity (MΩ·cm)	TOC (ppb)	Temperature (ºC)
4.8	18.2	2	19.7

4.2.2. Real matrix water

All the matrices used in the experiments were obtained from the output of four different secondary treatments from the water treatment plants of Gavà-Viladecans and El Prat de Llobregat.

4.2.2.1. Integrated fixed-film activated sludge (IFAS) biological reactor treatment water.

The IFAS process consists in the degradation of the organic matter of the wastewater by attacks of the aerobic bacteria. The biomass of the reactor can be found in suspension or adhered in the form of a biofilm in the walls of the reactor. This water comes from Gavà-Viladecans WWTP. [32]

Table 5. IFAS matrix characterization.

Propriety	pH	Turbidity (NTU)	Conductivity ($mS \cdot cm^{-1}$)	UV_{254} (m^{-1})	COD (mg $O_2 \cdot L^{-1}$)	TOC (mg $C \cdot L^{-1}$)
Value	7.8	18.5	2.19	50.30	71.32	51.11

DOC (mg C·L^{-1})	IC (mg C ·L^{-1})	Total alkalinity (mg Ca_2CO_3·L^{-1})	Cl^{-1} (mg·L^{-1})	SO_4^{2-} (mg·L^{-1})	$N\text{-}NO_2^-$ (mg·L^{-1})	$N\text{-}NO_3^-$ (mg·L^{-1})
21.66	121.60	469.41	543.00	196.80	0.16	0.27

4.2.2.2. With nutrients elimination treatment water (AEN).

In this treatment, it is intended to minimize the contribution of nutrients and thus achieve a 70% elimination of nitrogen and phosphorus. This water comes from El Prat de Llobregat WWTP.[33]

Table 6. AEN matrix water characterization.

Propriety	pH	Turbidity (NTU)	Conductivity (mS·cm^{-1})	UV_{254} (m^{-1})	COD (mg O_2 · L^{-1})	TOC (mg C · L^{-1})
Value	7.5	2.6	2.38	24.60	27.28	13.17

DOC (mg C·L^{-1})	IC (mg C ·L^{-1})	Total alkalinity (mg Ca_2CO_3·L^{-1})	Cl^{-1} (mg·L^{-1})	SO_4^{2-} (mg·L^{-1})	$N\text{-}NO_2^-$ (mg·L^{-1})	$N\text{-}NO_3^-$ (mg·L^{-1})
13.34	70.44	275.03	464.40	199.50	0.28	8.26

4.2.2.3. Without nutrients elimination treatment water (SEN).

The WTTP of El Prat de Llobregat have two water lines. In one line there is the secondary treatment AEN and in the other line this treatment without nutrients elimination.[33]

Table 7. SEN matrix characterization.

Propriety	pH	Turbidity (NTU)	Conductivity (mS·cm^{-1})	UV_{254} (m^{-1})	COD (mg O_2 · L^{-1})	TOC (mg C · L^{-1})
Value	8.0	20.1	2.71	48.90	70.46	37.85

DOC (mg C·L^{-1})	IC (mg C ·L^{-1})	Total alkalinity (mg Ca_2CO_3·L^{-1})	Cl^{-1} (mg·L^{-1})	SO_4^{2-} (mg·L^{-1})	$N\text{-}NO_2^-$ (mg·L^{-1})	$N\text{-}NO_3^-$ (mg·L^{-1})
18.67	123.70	449.08	486.00	175.20	0.12	0.30

4.2.2.4. Membrane Bioreactor (MBR) treatment water.

The operating principle of a membrane bioreactor is the same as an IFAS bioreactor. The difference lies in the solid-liquid separation method to obtain a clarified effluent because in this

treatment the separation is carried out by microfiltration or ultrafiltration membranes. The MBR water comes from Gavà-Viladecans.[32]

Table 8. MBR matrix characterization.

Propriety	pH	Turbidity (NTU)	Conductivity ($mS \cdot cm^{-1}$)	UV_{254} (m^{-1})	COD (mg $O_2 \cdot L^{-1}$)	TOC (mg $C \cdot L^{-1}$)
Value	7.7	0.5	2.52	17.40	14.92	13.56

DOC (mg $C \cdot L^{-1}$)	IC (mg $C \cdot L^{-1}$)	Total alkalinity (mg $Ca_2CO_3 \cdot L^{-1}$)	Cl^{-1} ($mg \cdot L^{-1}$)	SO_4^{2-} ($mg \cdot L^{-1}$)	$N\text{-}NO_2^-$ ($mg \cdot L^{-1}$)	$N\text{-}NO_3^-$ ($mg \cdot L^{-1}$)
13.34	53.56	208.31	565.20	187.80	0.19	8.40

4.3. **ANALYTICAL METHODS**

In this section are shown the different methods and measurements were employed:

4.3.1. High Performance Liquid Chromatograph (HPLC)

PROP concentration was analysed by HPLC working under following conditions:

- Column: SEA18 Teknokroma (250 x 4.6 mm i.d.; 5µm particle size).
- Pressure: 110 bars
- Mobile phase: Water:Acetonitrile (65:35)
- Flow-rate: 0.7 mL/min
- Detection: 214.4 nm

The instrumental used was HPLC 1260 Infinity from waters by Agilent Technologies.

4.3.2. Determination of iron species

Fe (II) was determined by the 1,10-phenantroline colorimetric method according to the International Organization for Standardization 1988 (ISO6332). In this method the ion Fe (II) is related to the absorbance of the orange-coloured complex created between 1,0-phenantroline and Fe(II) at 510 nm wavelength.

$$Fe\ (II) + 3\ Phen \longrightarrow [Fe(Phen)_3]^{2+}$$

Iron total, both Fe (II) and Fe (III), was determined by the same method but reducing the Fe (II) with ascorbic acid. Finally, Fe (III) was calculated by difference between total iron and Fe (II).[34]

4.3.3. Determination of hydrogen peroxide consumption

Hydrogen peroxide concentration was determinated by metavanadates procedure and measured by Hach Lange DR 3900 spectrophotometer. In this method the reaction taking place the proxovanadium ion formation with its maximum absorption at 450 nm.[35]

$$VO_3^- + 4H^+ + H_2O_2 \longrightarrow 3H_2O + VO_2^{3+}$$

4.3.4. Determination of Chemical Oxygen Demand (COD)

The chemical oxygen demand (COD) measures the equivalent oxygen to the organic matter which is susceptible to be oxidized by a specific and strong chemical agent working under accurate temperature and time conditions. The amount of oxidant consumed is expressed in terms of its oxygen equivalence (mg O_2/L).

The analysis was done according the ASTM D1252-06 Standard Test Methods for COD (Dichromate Oxygen Demand) of Water and it consisted of sample oxidation with a certain amount of potassium dichromate in excess, it was carried out in an acid medium, with catalysts and at 150ºC for 2h.

There are two sorts of COD measurements, high and low range. Low-range COD is used for concentrations lower than 100 mg O_2/ L and the initial dichromate decrease is measured by spectrophotometry at a wavelength of 420 nm. For high-range COD (concentrations from 0 to 1000 mg O_2/ L) the spectrophotometric reading is performed at 600 nm.[36]

4.3.5. Determination of Biochemical Oxygen Demand (BOD_5)

In an analogous way to the COD, the analytical technique of the biological determination of oxygen (BOD_5) measures the requirement of oxygen for the degradation of the organic matter but, unlike the COD, the degradation is done by microorganisms and metabolic activities.

The BOD_5 was done according the 5210-standard method that consisted of filling with seeded and nourished sample an airtight bottle of specified size, which is incubated it at the specified temperature for 5 days. The measurement was done by OxyTop whose mechanism is based on

variation the pressure in a closed system. The microorganisms that are in the sample consume oxygen and generate CO_2 because of their metabolic activity. This CO_2 is absorbed with NaOH and then a pressure decrease is produced, which is related to oxygen concentration and BOD.

4.3.6. Total Organic Carbon (TOC)

Total organic carbon (TOC) is the amount of carbon found in an organic compound and it is often used as a parameter to check the quality of the water during the water purification process.

The TOC analysis was done according to 5220D-standard method that consisted in a catalytic combustion at 680ºC. It was performed with Shimadzu 5055 TOC-VCSN analyser with an ASI-V Autosampler.

4.3.7. pH measurement

The pH reading was performed by CRISON GLP 22 pH meter correctly calibrated each day with pH 7.0 and pH 4.0 buffers.

4.3.8. Turbidity

The values of turbidity in water matrices were measured by 2100P turbidimeter.

4.3.9. Conductivity

The values of conductivity in water matrices were measured by CRISON GLP 22.

4.3.10. Biodegradability

The ratio between BOD_5 and COD is the biodegradability. The value of this ratio will be in a range from 0 to 1 and values closer to 1 indicates that the water have most biodegradability.

$$\text{Biodegradability} = BOD_5/COD$$

4.4. EXPERIMENTAL DEVICE

The experiments were carried out in a jacketed batch reactor made of Pyrex, with a volume of 2L, 23 cm height and 11 cm of inner diameter. The jacket is connected to a thermostatic bath to maintain the temperature at 25ºC.

In the first type of experiments, the light source employed was BLB Philips TL 8W-08 FAM with 8W power and located at the centre of the reactor inside a Pyrex sheath. The BLB radiation range was from 300 nm to 410 nm having the maximum of light emission at 365 nm. This lamp had 10,000 hours lifetime.

On the other hand, eight TSLC N3535 UVA-LED were used with 1.05 W of power each and 365±5 nm of wavelength, LEDs were located inside the same sheath that BLB lamp. LED life time was 26,000 hours.[28]

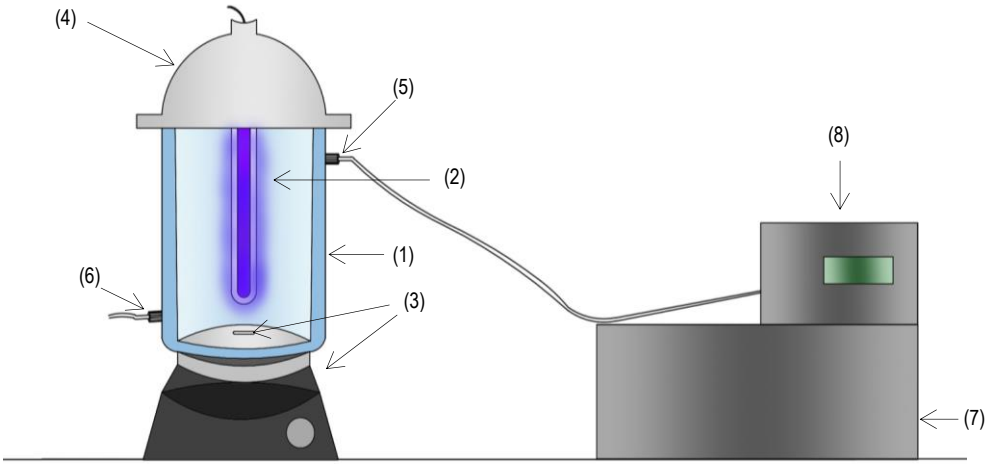

Figure 5. Reactor Device. (1) 2L jacketed reactor, (2) BLB /LED lamp, (3) Magnetic stirrer, (4) Alumina foil, (5) Thermostatic bath (IN), (6) Thermostatic bath (OUT), (7) Thermostatic bath and (8) Thermostatic bath temperature controller. Source: Autocad and SketchBook from Autodesk.

4.5. **EXPERIMENTAL PROCEDURE**

Table 9. Degradation and COD results of the experiments. All of them were performed at pH=2.6±0.2, 50 ppm of PROP, 150 ppm of H_2O_2 and 10 ppm of Fe(II). BLB light were employed to experiments 1-9 and LED to experiments 10-16.

Experiment	Matrix	Degradation (%)	COD (%)
Experiment 1	IFAS	69.20	-
Experiment 2	IFAS	68.50	-
Experiment 3	SEN	83.52	-
Experiment 4	Milli-Q	100.00	78.99
Experiment 5	MBR	95.28	39.19
Experiment 6	IFAS	73.06	0.00
Experiment 7	SEN	83.98	13.68
Experiment 8	AEN	71.87	13.46
Experiment 9	AEN	65.50	0.00
Experiment 10	Milli-Q	100.00	13.46
Experiment 11	IFAS	32.91	0.00
Experiment 12	AEN	50.53	10.53
Experiment 13	MBR	52.08	-
Experiment 14	SEN	40.20	1.02
Experiment 15	MBR	51.81	19.62
Experiment 16	AEN	55.18	10.42

The PROP degradation by photo-Fenton was measured for one hour using the optimal ratio Fe(II)/H_2O_2 (0.07 in ppm) with 10 ppm Fe(II) and 150 ppm H_2O_2 concentrations. [37]

In the minutes 0, 0.5, 2, 4, 5, 10, 15, 20, 30, 45 and 60 samples were taken from inside of reactor. For each sample, 0.5 mL was inverted for HPLC, 5 mL for determination of COD and UV-254, 4 mL for Fe(II) and total iron progression and 1.5 mL for H_2O_2 progression. At the end of each experiment, 1L of sample was taken for the BOD_5 analysis.

Every experiment had the following procedure:

1. Pre-treatment of the water from the WWTP, which consisted of filtering 2.5 L of water with a vacuum pump and a Büchner funnel. Except experiments with Milli-Q matrix.
2. Water was temperate until reaching the ambient temperature because the water from the WWTP was stored at low temperatures. Except experiments with Milli-Q water.
3. Lowered water pH to 2.6±0.2 using H_2SO_4.
4. Preparation of the solution of PROP and $FeSO_4 \cdot 7H_2O$, 0.1 g of PROP and 0.1 g of $FeSO_4 \cdot 7H_2O$ were weighed and dissolved with water in a 2L volumetric flask.
5. Agitation and homogenization of the solution with a magnetic stirrer during 20 minutes.

6. Activation of thermostatic bath at an operating temperature of 25ºC.
7. Introduction of the solution in the reactor with stirring at 500 rpm.
8. For the experiments that were carried out with BLB light, the lamp was switched on 15 minutes before the start of the reaction.
9. The reaction was initiated with the injection of 1 mL of H_2O_2 into the reactor. Sample were taken during the experiment at minutes 1, 2, 4, 5, 10, 15, 20, 30, 45 and 60.
10. During the experiment, the monitoring of Fe (II) and H_2O_2 of each sample was carried out.
11. At 60 minutes, the experiment finalized, turning off the light, disconnecting the thermostatic bath and stopping the agitation.
12. The 11 samples collected during the experiment were basified with 0.1M NaOH until reaching a pH in a range of 6.5 to 7.5. This was necessary because subsequently 5 drops of a bovine catalase solution were added to stop the reaction.
13. Analogously to step 11, at the end of the experiment, 1L of the reactor solution was collected at which the pH was raised to 6.5-7.5 and 5 mL of bovine catalase was added.
14. At the time when bovine catalase was added (steps 11 and 12) the chronometer was started and after 15 minutes it was verified that there was no H_2O_2 in the sample. For the test, H_2O_2 test strips were used, which by colour indicated the presence or not of H_2O_2. In the case that there was still H_2O_2, a small amount of catalase should be added, and the procedure of this step was repeated.

5. RESULTS AND DISCUSSION

5.1. BLB LIGHT REACTOR

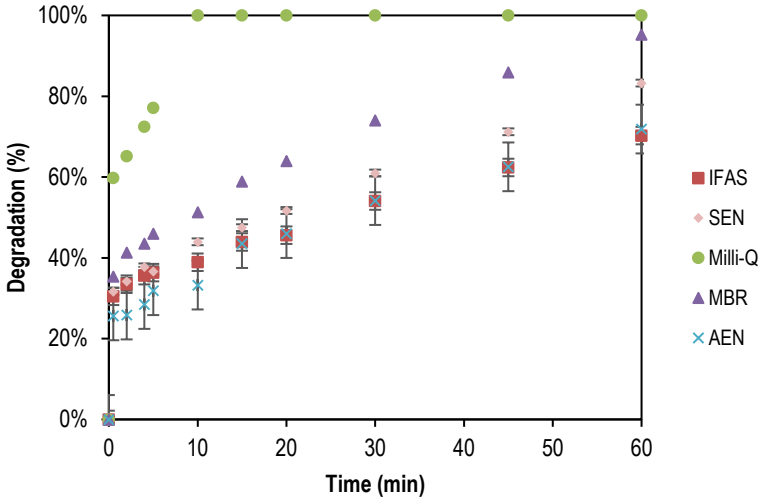

Figure 6. Degradation with BLB light source. Photo-Fenton experiments with 50 ppm of PROP, 10 ppm of Fe(II) and 150 ppm of H_2O_2.

Figure 6 shows the degradation percentages of the PROP obtained in the BLB light source experiments for each type of matrix. It is observed that the matrix corresponding to Milli-Q water shows the highest degradation (100% in 10 minutes). The justification lies in the fact that the Milli-Q water, being ultrapure, has a very small TOC value (2 ppb), consequently only the presence of our contaminant exists in the water, accordingly the photo-Fenton reaction degrades only the pollutant and does not interact with the matrix.

The MBR matrix presents a final percentage of degradation of 95.28 followed by SEN with 83.75±0.003%, AEN with 76.79±0.07% and, finally, IFAS with a 70.25±0.02%. Regarding the degradation of PROP in the waters coming from WWTP, several factors must be considered, such as the presence of organic compounds and ions in these waters.

Analysing the values corresponding to the dissolved organic carbon in the different matrices, DOC decreases following the order: IFAS, AEN, SEN, and MBR. This expected order is due to the fact that the highest values of DOC in the matrix indicate more quantity of organic compounds

and, considering that the photo-Fenton reaction is not selective, organic compounds of the matrix compete with PROP for hydroxyl radicals. Consequently, less percentage of PROP degradation was achieved when more DOC was present.

On the other hand, the effect of the ions present in the water influences the reaction so that the scavenger effect can happen. The scavenging effect refers to the ability of many antioxidants to act as stabilizers or inhibitors of various reactive species. In the case of free radicals, such action implies its stabilization through the assignment of an electron to these reactive molecules, so that there is an inhibition of degradation rate of target pollutant due to of the disappearance of hydroxyl radicals. In the case of our matrices, the Cl^-, SO_4^{2-}, NO_2^- and NO_3 will be the cause of the scavenger effect. Therefore, the higher the concentration of these ions (Figure 7), the higher the scavenging effect of the hydroxyl radicals and the lower the degradation obtained. With all this,e expected is that the order of degradation from highest to lowest is MBR, AEN, SEN and IFAS respectively.[38]

If we compare the results obtained experimentally with the expected according to the theoretical concepts we see that the predictions are fulfilled.

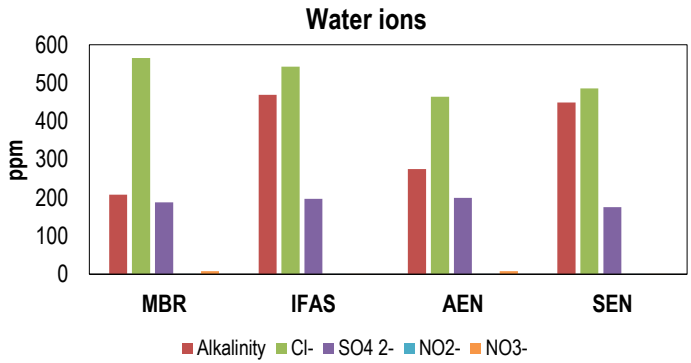

Figure 7. Ions concentrations in different matrices.

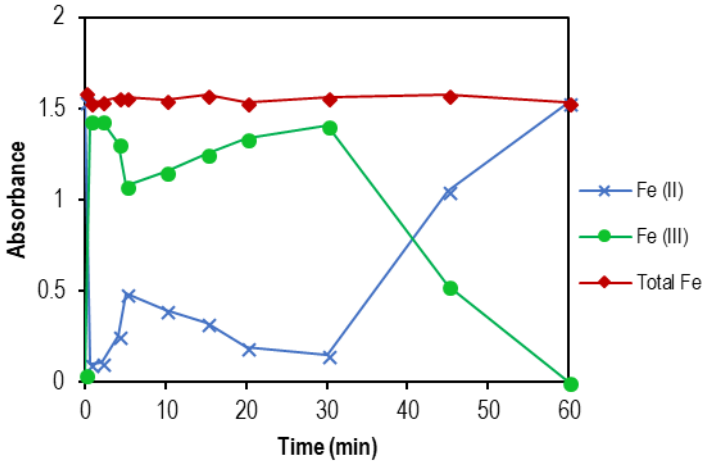

Figure 8. Iron progression during the experiment in Milli-Q matrix, BLB light source and 50 ppm of PROP, 10 ppm of Fe(II) and 150 ppm of H_2O_2.

As shown in Figure 8, iron ions evolve during the photo-Fenton reaction in such a way that Fe (II), which acts as a catalyst, is initially consumed to form Fe (III) and radicals $HO^{\bullet}$ (Eq.2.1 and Eq.2.2) until 30 minutes of reaction when begins its regeneration due to the interaction of Fe (III) with the peroxide (Eq.2.3, Eq.2.4 and Eq.2.5). It is observed how the total iron remains constant during the reaction, which indicates that the iron has not precipitated during the process.

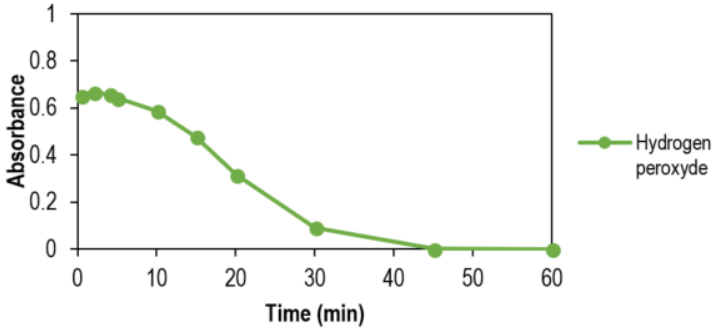

Figure 9. Hydrogen peroxide evolution during the experiment in Milli-Q matrix, BLB light source and 50 ppm of PROP, 10 ppm of Fe(II) and 150 ppm of H_2O_2.

In turn, in Figure 9, it can be seen how hydrogen peroxide is consumed throughout the experiment as it acts as a reactant in the photo-Fenton process.

Figures 8 and 9 correspond to experiment number 3 whose matrix used was Milli-Q. This experiment has been chosen because there are no interactions with the matrix.

5.2. **LED LIGHT REACTOR**

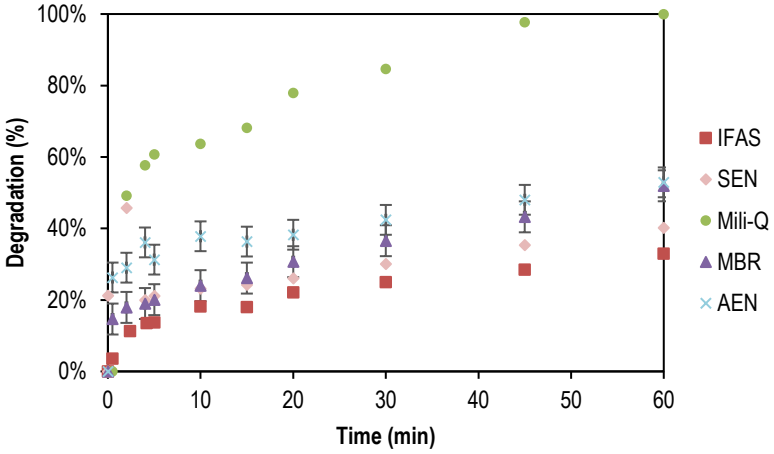

Figure 10. Degradation in LED light source photo-Fenton experiments with 50 ppm of PROP, 10 ppm of Fe(II) and 150 ppm of H_2O_2.

We see (Figure 10) that the degradation values are lower with respect to the values obtained for BLB. The results were: 100% for Milli-Q (in 45 minutes), 51.94 ±0.10% for MBR, 52.91±0.04% for AEN, 40.20% for SEN and 32.91% for IFAS.

As it has been observed in the values obtained for degradation of the PROP in the matrices MBR, SEN and AEN, these do not follow the same order for BLB as for LED. The justification is due to the main difference found in the characterization of AEN respect to SEN is its alkalinity. Therefore, when working at acidic pH, the alkalinity of water disappears becoming MBR, SEN and AEN into three very similar water matrices. For this reason, the percentage values between them do not differ by more than 15%.

The justification for the degradation values with LED lower than those obtained in BLB resides in the radiation emitting reactor used. While in the BLB light source the angle of light emission is 360º for the LED light the angle is 120º. Thus, we have a model of continuous light radiation (BLB) were the light arrives homogeneously to the reactor. On the other hand, for the LED light source is not continuous, being punctual sources of light, which causes dark zones in the reactor. That is why we must emphasize the importance of the radiation model in photochemical reactions.

Studies in our research group show that, under equal conditions and with a geometry in which the location of the LEDs allows to have the emission model approximated at the BLB lamp, the degradation obtained for the LED reactor is greater than that obtained for BLB.

Figure 11 shows the results in diphenydramine hydrochloride (DPH) degradation performed in a 0.5L reactor with 4W power for BLB and LED. In these experiments having lower reaction volume, dark areas are almost avoided so that LED and BLB give similar results. Thus, 100% degradation of DPH was obtained at 30 minutes for the LED reactor while at the same time a 99% degradation for BLB was obtained. These experiments confirm the importance of optimal geometry in the arrangement of light in photochemical reactions.

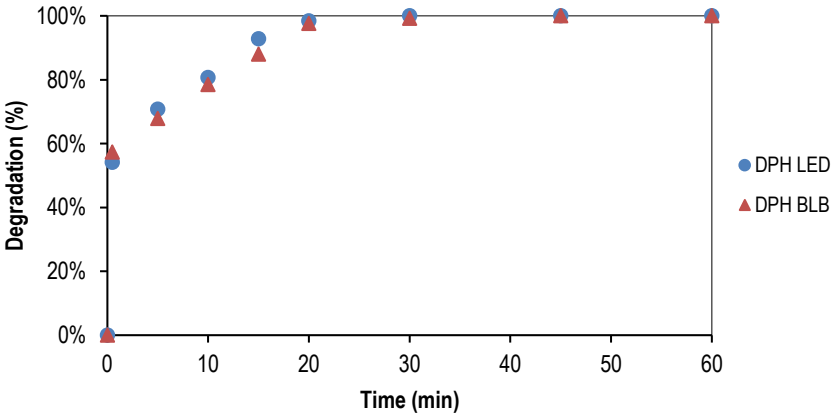

Figure 11. Comparison between LED and BLB sources working at 4W power in DPH degradation in Milli-Q water with 50 ppm of DPH, 10 ppm of Fe(II) and 150 ppm of H_2O_2 .

5.3. BIODEGRADABILITY, UV-254 AND COD

The oxidation percentages (Table 9) show that the order of highest and the lowest oxidation is the same as that corresponding to the order of percentage of degradation (Section 5.1 and 5.2). For the BLB light source the results were: Milli-Q 78.99%, MBR 39.19%, SEN 13.68%, AEN 13.46% and IFAS 0.00%. For the LED light the results were: Milli-Q 13.46%, MBR 19.62%, SEN 1.02%, AEN 10.48 and IFAS 0.00%. The study of these results indicates that the greater the degradation of the PROP contaminant, the greater the oxidation that occurs at the end of the photo-Fenton process.

The results corresponding to the BOD_5 values obtained at initial time (before starting the experiments) had a value between 0 and 1 mg O_2/L, indicating that the initial biodegradability was very low or practically nil. For these low values, the Oxytop could not be read because it was not precision enough.

The values of biodegradability at the end of the experiments in BLB light were: 0.443 for Milli-Q, 0.145 for IFAS, 0.120 for MBR, 0.085 for SEN and 0.078 for AEN. The results in LED light were: 0.111 for Milli-Q, 0.066 for MBR, 0.062 for SEN, 0.059 for AEN.

Values of MBR, IFAS, SEN and AEN are lower. In the same way as in the justification of section 5.2, the three values are very close again.

The biodegradability values obtained in LED are lower than those obtained in BLB because in all the matrices there is less PROP degradation, resulting in a lower appearance of reaction intermediates.

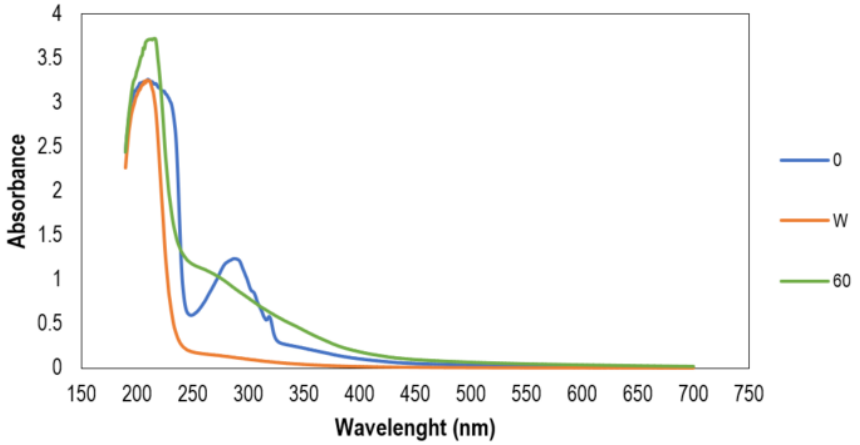

Figure 12. Spectrum of experiment 5 in MBR matrix, BLB light source and 50 ppm of PROP, 10 ppm of Fe(II) and 150 ppm of H2O2. W: water spectrum without PROP, 0: water spectrum at initial experimental time. 60: water spectrum at final experimental time.

Figure 12 shows the absorption spectrum for a range of 190 to 700 nm wavelength. In this case, the spectrum of experiment 5 was selected in which the matrix used was MBR. The W series corresponds to the spectrum of water without contaminants, the 0 series corresponds to the MBR water spectrum with 50 ppm of PROP (before starting the experiment) and the 60 series corresponds to the water at the end of the experiment. We observed that one of the two peaks corresponding to PROP (288 nm) decreases at the end of the experiment, which indicates that degradation occurs. Now, if we look at the wavelength 254 nm, which corresponds to the absorption of aromatics, we see that it increases at the end of the experiment. This is explained by the formation of intermediates in the course of the reaction whose aromaticity is higher than PROP. By performing a literature search, they have been found possible intermediates produced in the degradation of the PROP in Milli-Q water matrix. They are show in Table 10.

Table 10. Possible intermediates formed in PROP degradation in Milli-Q water.[20]

Compound	Formula	Structure
A	$C_{16}H_{21}NO_2$	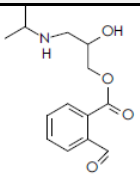
B	$C_{14}H_{19}NO_4$	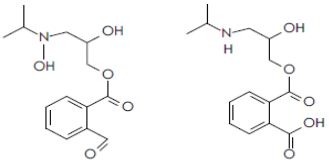 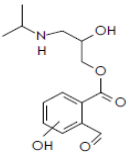
C	$C_{14}H_{19}NO_5$	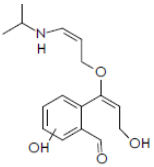 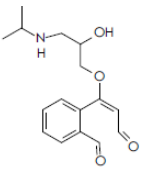
D	$C_{16}H_{21}NO_5$	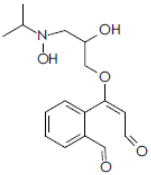 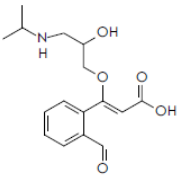
E	C_3H_7NO	
F	$C_6H_{11}N$	
G	$C_6H_{13}NO$	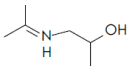
H	$C_6H_{15}NO_2$	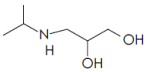
I	$C_6H_{15}NO_3$	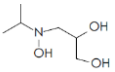

5.4. **EFFICIENCY CONSIDERATIONS**

For the estimation of the Energetic Efficiency (EE) in ppm·kW^{-1}·h^{-1}, the following equation has been used:

$$EE = (C_{PROP,o} - C_{PROP})/(P \cdot t)$$

P: nominal power (kW) $C_{PROP,o}$: initial concentration (ppm)

C_{PROP}: final concentration (ppm) t: 10 minutes.

In this case 10 minutes were selected because is the minimum time of PROP degradation (in Milli-Q water for BLB light source).

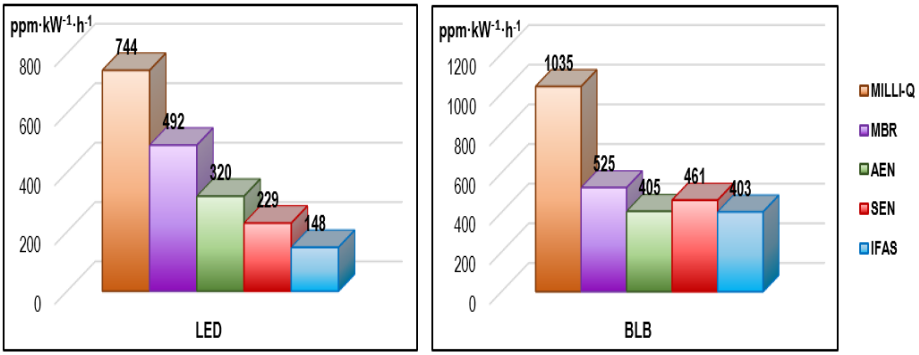

Figure 13. Efficiency results for each light source (BLB and LED) and each water matrix employed.

Higher values of EE indicate a lower energy consumption and therefore it is an indicator of highest efficiency. In the case of our experiments, we obtain higher efficiency in BLB than in LED (due to the radiation model discussed in section 5.2) and in matrices that have fewer ions and less DOC (justification in section 5.1).

5.5. KINETICS

The degradation reaction of PROP were fitted to pseudo first order kinetics using following equation:

$$C_{PROP}=C_{PROP,o}\cdot\exp(-k\cdot t)$$

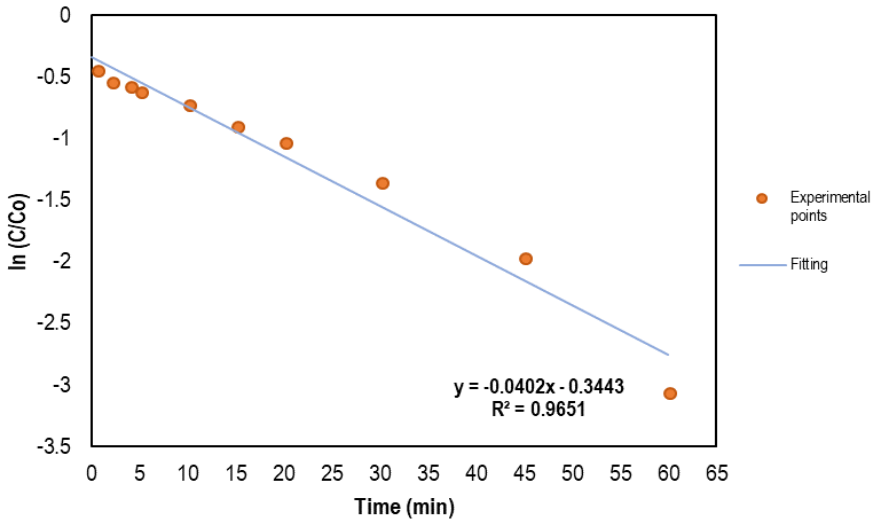

Figure 134. Kinetic linealization for Experiment 6 with MBR water and BLB light source.

Linearizing the equation (Figure 14), the value of the kinetic constant can be obtained from the slope of the linearization. The k values obtained, with its R^2, are shown in Table 11. For the replicated experiments the average and the standard deviation were calculated.

Table 11. Kinetics results for each water matrix.

Matrix	Light	V_o (ppm/min)	k (min^{-1})	R^2
Milli-Q		59.33	0.1234	0.9852
MBR		34.77	0.0402	0.9651
AEN	BLB	25.44	0.0141±0.0030	0.9888
SEN		40.48	0.0204±0.0016	0.9885
IFAS		30.37	0.0138±0.0010	0.9832

Milli-Q		42.22	0.1351	0.9161
MBR		8.03	0.0088±0.0003	0.9965
AEN	LED	21.46	0.0071±0.0003	0.9479
SEN		20.15	0.0049	0.9898
IFAS		2.84	0.0051	0.9054

According to the vàlues of the degradation, the highest kinetic constant was obtained for the matrix corresponding to Milli-Q water, both with BLB and LED lamps. It was expected because, in this case, there is not competence from the organic matter as it occurs in the other matrices tested.

6. CONCLUSIONS

- Concerning the water matrix influence on the degradation of PROP by photo-Fenton, the lowest degradation was obtained with the matrix IFAS, because it has the highest content of organic matter and ions.
- The comparison between LEDs and BLB is possible only related to the electrical efficiency because the radiation models are different. In this way the highest efficiency was obtained with BLB lamps and Milli-Q water matrix.
- The biodegradability depends on the percentage of PROP degradation and the formation of reaction intermediates. The most biodegradable water after the photo-Fenton process is always the Milli-Q water. The values of COD have the same tendency because the presence of more organic matter and ions inside the water matrix produces smaller oxidation. Thus, the water with less oxidation is the IFAS matrix.
- The aromaticity increases at the end of each experiment. During the PROP degradation, reaction intermediates appear that absorb at 254 nm wavelength, indicating aromaticity.
- The highest reaction rate and kinetic constant correspond to the PROP degradation with BLB lamps in Milli-Q water.

REFERENCES AND NOTES

1. Gude,V. Desalination and water reuse to address global water scarcity. *Reviews in Environmental Science and Biotechnology*. **2017,** *16,* 591-609.
2. Informe Sequía algo más que la falta de Lluvia. Impactos e imágenes. *Geenpeace*. **2017**.
3. United Nations. World Water Development Report **2018**, Geneva, Switzerland.
4. Richardson, S.; Kimura,S. Emerging environmental contaminants: Challenges facing our next generation and potential engineering solutions*. Environmental Technology and Innovation.* **2017,** *8,* 40-56.
5. Geissen, V.; Mol, H.; Klumpp, E.; Umlauf, G.; Nadal, M.; Van Der Ploeg, M.; Van De Zee, E.A.T.M.S.; Ritsema, C.J. Emerging pollutants in the environment: A challenge for water resource management. *International Soil and Water Conservation Research.* **2015,** 57-65.
6. Monograph Propanolol Hydrichloride. *The American Society of Health-System Pharmacists.* **2015**, https://www.drugs.com/monograph/propranolol-hydrochloride.html (accessed March 9, 2018).
7. Moraes, M.; Grings, A.; Pereira, B.; Leite, R.D.; Vieira, A.; De Sousa, N.M.F; Simão, R.; Prestes, J. Different Cardiovascular Responses to a Resistance Training Session in Hypertensive Women Receiving Propranolol Compared with Normotensive Controls. *The Scientific World Journal.* **2012,** 1-6.
8. Bauman, N. Propranolol effectively treats significant infantile hemangiomas. *Journal of Pediatrics.* **2015,** https://doi.org/10.1016/j.jpeds.2015.04.089 (accessed March 9, 2018).
9. Ruiz, R.; Ávila, R.; González, J.A. Enantiomeric separation and quantitative determination of propranolol enantiomers in pharmaceutical preparations by chiral liquid chromatography. *Brazilian Journal of Pharmaceutical Sciences.* **2004,** *40*, 3.
10. File: PropranololEnantiomers.png. **2008,** https://commons.wikimedia.org/wiki/File:Propranolol_Enantiomers.png. (accessed March 10, 2018).
11. Directive 2000/60/EC of the European Parliament and of the Council of 23 October 2000 establishing a framework for Community action in the field of water policy. *Official Journal (OJ L 327).* **2000**.
12. Decision No 2455/2001/EC of the European Parliament and of the Council of 20 November 2001 establishing the list of priority substances in the field of water policy and amending Directive 2000/60/EC. *Official Journal (OJ L 327).* **2001**.
13. Directive 2013/39/EU of the European parliament and of the council of 12 August 2013 amending Directives 2000/60/EC and 2008/105/EC as regards priority substances in the field of water policy.
14. De Luca, A.; Dantas, R.; Simoes, A.S.M.; Toscano, I. A. S.; Lofrano, G.; Cruz, A.; Esplugas, S. Atrazine removal in municipal secondary effluents by Fenton and photo-Fenton Treatments. *Chemical Engineering Technology. 36*, 2155-2162.
15. Dewil, R.; Mantzavinos, D.; Poulios, I.; Rodrigo, M. A. New perspectives for Advanced Oxidation Processes. *Journal of Environmental Management.* **2017,** *195*, 93-99.
16. Deng, Y.; Zhao, R. Advanced Oxidation Processes (AOPs) in Wastewater Treatment.
17. Liu, J.; Ye, J.; Chen, Y.; Li, C.; Ou, H. UV-driven hydroxyl radical oxidation of tris(2-chloroethyl) phosphate: Intermediate products and residual toxicity. *Chemosphere.* **2018,** *190*, 225-233.
18. Gupta, S.; Basant, N. Modelling the aqueous phase reactivity of hydroxyl radical towards diverse organic micropollutants: An aid to water decontamination processes. *Chemosphere.* **2017,** *185*, 1164-1172.
19. López, N. Heterogeneous photocatalytic degradation over titanium dioxide of toluene in gas phase and Diphenhydramine in liquid phase. *Master Final Project, Master of Environmental Engineering Universitat de Barcelona.* **2016**
20. De la Cruz, N. Estudio de la eliminación de contaminantes emergentes en aguas mediante Procesos de Oxidación Avanzados. *Doctoral thesis, Advanced Oxidation Group Universitat de Barcelona.* **2013**.

21. Carra, I.; Sánchez, J. A.; Malato, S.; Oliver, A.; Bruce, J.; Jarvis, P. Application of high intensity UVC-LED for the removal of acetamiprid with the photo-Fenton process. *Chemical Engineering Journal*. **2015,** *264*, 690-696.
22. Verma, S.; Sillanpää, M. Degradation of anatoxin-a by UV-C LED and UV-C LED/H2O2 advanced oxidation processes. *Chemical Engineering Journal.* **2015,** *274*, 274-281.
23. Würtele, M.A.; Kolbe, T.; Lipsz, M.; Külberg, A.; Weyers, M.; Kneissl, M.; Jekel, M. Application of GaN-based ultraviolet-C light emitting diodes-UV-LEDs-for water disinfection. *Water Research*. **2011,** *45*, 1481-1489.
24. Moreira, N. F. F.; Sousa, J. M.; Macebo, G.; Ribeiro, A.; Barreiros, L.; Pedrosa, M.; Faria, J.; Pereira, M.F.R.; Castro-Silva, S.; Segundo, M.A.; Manaia, C.M.; Nunes, O.; Silva, A. Photocatalytic ozonation of urban wastewater and surface water using immobilized TiO2 with LEDs: Micropolutants, antibiotic resistence genes and estrogenic activity. *Water Research.* **2016,** *94*, 10-22.
25. Gil, E.; Dobrosz, I.; Gómez, M.A. Coagulation-flocculation sequential with Fenton or Photo-Fenton processes as an alternative for the industrial textile wastewater treatment. *Journal of Environmental Management.* **2017,** *191*, 189-197.
26. Rodrigues, C. Optimization and economic analysis of textile wastewater treatment by photo-fenton process under artificial and simulated solar radiation. *Industrial & engineering chemistry research.* **2013,** *52*, 133,13-13324.
27. Han Tran, N.; Reinhard, M.; Yew-Hoong Gin, K. Occurrence and fate of emerging contaminants in municipal wastewater treatment plants from different geographical regions-a review. *Water Research*. **2018,** *133*, 182-207.
28. G. Matafonova, V. Batoev. Recent advances in application of UV light-emitting diodes for degrading organic pollutants in water through advanced oxidation processes: A review. *Water Research*. **2018,** Vol.132, 177-189.
29. PubChem database. https://pubchem.ncbi.nlm.nih.gov/. (Accessed March 10, 2018).
30. Propranolol hydrochloride. ChemIDplus. https://chem.nlm.nih.gov/chemidplus/sid/0000318989. (Accessed March 18, 2018).
31. Milli-Q. https://en.wikipedia.org/wiki/Milli-Q. (Accessed March 21, 2018).
32. GEDAR. Gestión de Aguas y Residuos. https://www.gedar.com/residuales/tratamiento-biologico-aerobio/bioreactor-membrana-mbr.htm. (Accessed March 22, 2018).
33. EDAR del Prat de Llobregat. http://www.amb.cat/es/web/medi-ambient/aigua/instalacions-i-equipaments/detall/-/equipament/edar-del-prat-de-llobregat/276285/11818. (Accesed March 22, 18).
34. American Public Health Association, American Water Works Association, Water Environment Federation. Standard Methods for the Examination of Water and Wastewater, **1999.**
35. Nogueira, R.; Oliveira, M.; Paterlini, W. Simple and fast spectrophotometric determination of H_2O_2 in photo-Fenton reactions using metavanadate. *Talanta.* **2005**, *66*, 86-91.
36. Lauber, F. Manual de procedimientos analíticos para muestras ambientales. Determinación de Demanda Química de Oxígeno en efluentes domésticos e industriales líquidos, aguas contaminadas y naturales. 2009UY. Método espectrofotométrico, reflujo cerrado. *DINAMA*. **2017.**
37. Abdulah Sayid, S.H.Y.; Abu Hassan, M.A.; Zainon Noor, Z.; Aris, A. Optimization of photo-Fenton oxidation of sulfidic spent caustic by using response surface methodology. *Department of Chemical Engineering, Faculty of Chemical Engineering, Universiti Teknologi Malaysia, Skudai, Johor,Malaysia. Institute of Environmental and Water Resource Management (IPASA). Universiti Teknologi Malaysia, Skudai, Johor, Malaysia.* **2011.**
38. Nakatani, N.; Hashimoto, N.; Shindo, H.; Masatoshi, Y.; Megumi, K.; Hiroshi, S. Determination of photoformation rates and scavenging rate constants of hydroxyl radicals in natural waters using an automatic light irradiation and injection system. *Analytica Chimica Acta.* **2007,** *581*, 260-267.

ACRONYMS

(ABPI) Association of British Pharmaceutical Industry

(AOPs) Advanced Oxidation Processes

(BOD) Biochemical Oxygen Demand

(BLB) Black Light Blue lamps

(COD) Chemical Oxygen Demand

(DOC) Dissolved Organic Carbon

(DPH) Diphenydramine hydrochloride

(ECs) Emergent Contaminants

(EE) Electrical Efficiency

(IC) Inorganic Carbon

(IFAS) Integrated Fixed-film Activated Sludge

(LED) Light-Emitting Diode

(MBR) Membrane Bioreactor

(ppb) Part per billion

(ppm) Part per million

(PROP) Propranolol

(POA) Processos d'Oxidació Avançada

(TOC) Total Organic Carbon

(WFD) Water Framework Directive

(WWTP) Waste Water Treatment Plant

APPENDICES

APPENDIX 1: RESULTS OF DEGRADATION, UV-254, IRON, HYDROGEN PEROXIDE AND COD FOR EACH EXPERIMENT.

The results of the degradation, the absorbance of all the iron species and hydrogen peroxide and the UV-254 and COD values obtained for each experiment are shown below. All the experiments were carried out at pH 2.6±0.2 and with concentrations of 50 ppm of PROP, 10 ppm of Fe (II) and 150 ppm of H_2O_2.

Table 12. Experiment 1 results. Matrix: IFAS and light source: BLB.

Time (minutes)	Degradation %	Absorbance					COD (ppm)
		Fe (II)	Fe (III)	Total iron	Hydrogen peroxide	UV-254	
0	0.00%	1.302	0.224	1.526	-	1.190	-
0.5	32.83%	0.185	1.114	1.299	0.639		
2	30.69%	0.222	1.245	1.467	0.677		
4	33.33%	0.184	1.259	1.443	0.696		
5	33.78%	0.172	1.297	1.469	0.659		
10	37.10%	0.137	1.285	1.422	0.528		
15	40.91%	0.176	1.283	1.459	0.585		
20	44.51%	0.089	1.334	1.423	0.550		
30	49.97%	0.204	1.239	1.443	0,530		
45	62.20%	0.221	1.216	1.437	0.541		
60	69.20%	0.222	1.070	1.292	0.528	0.054	-

Table 13. Experiment 2 results. Matrix: IFAS and light source: BLB.

Time (minutes)	Degradation %	Absorbance					COD (ppm)
		Fe (II)	Fe (III)	Total iron	Hydrogen peroxide	UV-254	
0	0.00%	1.328	0.245	1.573	-	1.190	-
0.5	32.83%	0.187	1.356	1.543	0.678		
2	35.39%	0.159	1.368	1.527	0.665		
4	35.99%	0.190	1.344	1.534	0.652		
5	36.72%	0.138	1.271	1.409	0.649		
10	38.89%	0.134	1.302	1.436	0.659		

15	44.91%	0.144	1.215	1.359	0.646		
20	44.69%	0.151	1.324	1.475	0.617		
30	57.69%	0.208	1.310	1.518	0.612		
45	62.23%	0.198	1.272	1.470	0.609		
60	68.49%	0.215	1.280	1.495	0.550	0.402	-

Table 14. Experiment 3 results. Matrix: SEN and light source: BLB.

Time (minutes)	Degradation %	Absorbance					COD (ppm)
		Fe (II)	Fe (III)	Total iron	Hydrogen peroxide	UV-254	
0	0.00%	1.293	0.171	1.464	-	0.839	-
0.5	30.77%	0,347	1.103	1.450	0.658		
2	33.80%	0.290	1.136	1.426	0.702		
4	39.14%	0.276	1.110	1.386	0.718		
5	37.21%	0.259	1.236	1.495	0.710		
10	43.26%	0.289	1.104	1.393	0.702		
15	48.08%	0.375	1.080	1.455	0.686		
20	52.02%	0.381	1.072	1.453	0.641		
30	60.27%	0.393	1.076	1.469	0.621		
45	70.96%	0.354	1.101	1.455	0.644		
60	83.52%	0.275	1.132	1.407	0.599	1.278	-

Table 15. Experiment 4 results. Matrix: Milli-Q and light source: BLB.

Time (minutes)	Degradation %	Absorbance					COD (ppm)
		Fe (II)	Fe (III)	Total iron	Hydrogen peroxide	UV-254	
0	0.00%	1.544	0.047	1.591	-	0.526	127.80
0.5	59.74%	0.103	1.434	1.537	0.653		
2	65.15%	0.104	1.437	1.541	0.665		
4	72.47%	0.252	1.307	1.559	0.658		
5	77.14%	0.487	1.078	1.565	0.643		
10	100.00%	0.392	1.157	1.549	0.588		
15	100.00%	0.327	1.252	1.579	0.477		
20	100.00%	0.192	1.339	1.531	0.317		
30	100.00%	0.151	1.410	1.561	0.091		
45	100.00%	1.047	0.526	1.573	0.0006		
60	100.00%	1.532	0	1.532	0	0.636	26.85

Table 16. Experiment 5 results. Matrix: MBR and light source: BLB.

Time (minutes)	Degradation %	Absorbance					COD (ppm)
		Fe (II)	Fe (III)	Total iron	Hydrogen peroxide	UV-254	
0	0.00%	1.348	0.164	1.512	-	0.632	96.00
0.5	35.39%	0.207	1.198	1.405	0.705		

2	41.31%	0.179	1.291	1.470	0.735		
4	43.53%	0.210	1.196	1.406	0.737		
5	45.99%	0.158	1.303	1.461	0.738		
10	51.27%	0.154	1.323	1.477	0.730		
15	58.88%	0.164	1.219	1.383	0.720		
20	64.00%	0.171	1.323	1.494	0.704		
30	74.03%	0.228	1.218	1.446	0.666		
45	85.94%	0.218	1.254	1.472	0.680		
60	95.28%	0.235	1.088	1.323	0.645	1.149	58.38

Table 17. Experiment 6 results. Matrix: IFAS and light source: BLB.

Time (minutes)	Degradation %	Absorbance					COD (ppm)
		Fe (II)	Fe (III)	Total iron	Hydrogen peroxide	UV-254	
0	0.00%	0.840	0.549	1.389	-	0.753	99.00
0.5	25.77%	0.745	0.708	1.453	0.630		
2	34.34%	0.797	0.663	1.460	0.648		
4	37.44%	0.809	0.639	1.448	0.655		
5	38.51%	0.755	0.702	1.457	0.649		
10	40.72%	0.796	0.672	1.468	0.652		
15	45.94%	0.834	0.577	1.411	0.628		
20	47.61%	0.619	0.694	1.313	0.605		
30	54.52%	0.586	0.606	1.192	0.601		
45	62.66%	0.910	0.463	1.373	0.597		
60	73.06%	1.009	0.423	1.432	0.573	1.103	99.00

Table 18. Experiment 7 results. Matrix: SEN and light source: BLB.

Time (minutes)	Degradation %	Absorbance					COD (ppm)
		Fe (II)	Fe (III)	Total iron	Hydrogen peroxide	UV-254	
0	0,00%	1,506	0,055	1,561	-	1.063	95.00
0.5	32,56%	0,621	1,07	1,691	0,559		
2	34,63%	0,63	0,906	1,536	0,777		
4	36,40%	0,65	0,915	1,565	0,762		
5	36,13%	0,615	0,948	1,563			
10	44,67%	0,614	0,912	1,526	0,758		
15	46,84%	0,669	0,863	1,532	0,758		
20	51,41%	0,681	0,902	1,583	0,752		
30	61,71%	0,693	0,835	1,528	0,723		
45	71,44%	0,768	0,731	1,499	0,699		
60	83,98%	0,830	0,680	1,510	0,660	1.250	82.00

Table 19. Experiment 8 results. Matrix: IFAS and light source: AEN.

Time (minutes)	Degradation %	Absorbance					COD (ppm)
		Fe (II)	Fe (III)	Total iron	Hydrogen peroxide	UV-254	
0	0.00%	1.565	0.000	1.564	-	0.807	104.00
0.5	25.63%	0.447	1.081	1.528	0.721		
2	25.83%	0.437	1.104	1.541	0.725		
4	28.44%	0.466	1.064	1.530	0.713		
5	31.86%	0.428	1.108	1.536	0.713		
10	33.25%	0.413	1.043	1.456	0.701		
15	43.52%	0.407	1.060	1.467	0.701		
20	46.00%	0.419	1.011	1.430	0.699		
30	54.17%	0.449	1.066	1.515	0.687		
45	62.53%	0.445	0.987	1.432	0.665		
60	71.87%	0.509	0.917	1.426	0.656	1.216	90.00

Table 20. Experiment 9 results. Matrix: AEN and light source: BLB.

Time (minutes)	Degradation %	Absorbance					COD (ppm)
		Fe (II)	Fe (III)	Total iron	Hydrogen peroxide	UV-254	
0	0.00%	1.510	0.088	1.598	-	1.106	101.00
0.5	32.51%	0.381	1.230	1.611	0.601		
2	34.03%	0.384	1.193	1.577	0.702		
4	35.11%	0.371	1.215	1.586	0.703		
5	38.31%	0.373	1.162	1.535	0.697		
10	41.03%	0.378	1.169	1.547	0.704		
15	42.36%	0.356	1.180	1.536	0.692		
20	45.67%	0.369	1.167	1.536	0.692		
30	54.73%	0.401	1.182	1.583	0.691		
45	62.58%	0.354	1.097	1.451	0.693		
60	65.50%	0.490	1.018	1.508	0.656	1.362	101.00

Table 21. Experiment 10 results. Matrix: Milli-Q and light source: LED.

Time (minutes)	Degradation %	Absorbance					COD (ppm)
		Fe (II)	Fe (III)	Total iron	Hydrogen peroxide	UV-254	
0	0.00%	1.266	0.266	1.532	-	0.825	104.00
0.5	49.19%	0.091	1.402	1.493	0.589		
2	57.65%	0.048	1.445	1.493	0.789		
4	60.70%	0.176	1.321	1.497	0.756		
5	63.66%	0.263	1.222	1.485	0.787		
10	68.17%	0.237	1.238	1.475	0.749		
15	77.93%	0.205	1.298	1.503	0.759		
20	84.66%	0.329	1.164	1.493	0.735		

30	97.73%	0.387	1.110	1.497	0.500		
45	99.92%	0.326	1.153	1.479	0.354		
60	100.00%	0.204	1.312	1.516	0.227	0.818	90.00

Table 22. Experiment 11 results. Matrix: IFAS and light source: LED.

Time (minutes)	Degradation %	Absorbance					COD (ppm)
		Fe (II)	Fe (III)	Total iron	Hydrogen peroxide	UV-254	
0	0.00%	1.109	0.387	1.496	-	0.256	94.00
0.5	3.62%	0.979	0.403	1.382	0.613		
2	11.28%	0.491	0.799	1.290	0.670		
4	13.54%	0.326	0.932	1.258			
5	13.74%	0.534	0.819	1.353	0.664		
10	18.17%	0.620	0.703	1.323	0.696		
15	18.02%	0.533	0.852	1.385	0.684		
20	22.08%	0.282	1.083	1.365	0.662		
30	25.02%	0.522	0.830	1.352	0.662		
45	28.44%	0.961	0.437	1.398	0.650		
60	32.91%	1.109	0.387	1.496		0.818	94.00

Table 23. Experiment 12 results. Matrix: AEN and light source: LED.

Time (minutes)	Degradation %	Absorbance					COD (ppm)
		Fe (II)	Fe (III)	Total iron	Hydrogen peroxide	UV-254	
0	0.00%	1.475	0.081	1.556	-	0.894	95.00
0.5	23.08%	0.457	1.063	1.520	0.586		
2	25.66%	0.527	1.006	1533	0.751		
4	26.46%	0.436	1.086	1522	0.749		
5	26.81%	0.445	1.083	1.,528	0.756		
10	38.44%	0.396	1.052	1.448	0.741		
15	33.53%	0.401	1.058	1.459	0.749		
20	35.74%	0.376	1.046	1.422	0.744		
30	40.10%	0.378	1.129	1.507	0.730		
45	44.61%	0.433	0.991	1.424	0.726		
60	50.63%	0.444	0.974	1.418	0.734	1.233	85.00

Table 184. Experiment 13 results. Matrix: MBR and light source: LED.

Time (minutes)	Degradation %	Absorbance					COD (ppm)
		Fe (II)	Fe (III)	Total iron	Hydrogen peroxide	UV-254	
0	0.00%	1.404	0.040	1.444	-	-	-
0.5	26.68%	0.245	1.101	1.346	0.725		

2	30.30%	0.302	1.239	1.541	0.744		
4	30.70%	0.302	1.207	1.509	0.766		
5	30.90%	0.325	1.214	1.539	0.748		
10	33.09%	0.308	1.143	1.451	0.743		
15	35.07%	0.354	1.126	1.480	0.738		
20	38.80%	0.452	1.074	1.526	0.709		
30	42.10%	0.390	1.138	1.528	0.735		
45	44.91%	0.339	1.177	1.516	0.722		
60	52.08%	0.339	1.201	1.540	0.728	-	-

Table 195. Experiment 14 results. Matrix: SEN and light source: LED.

Time (minutes)	Degradation %	Absorbance					COD (ppm)
		Fe (II)	Fe (III)	Total iron	Hydrogen peroxide	UV-254	
0	0.00%	1.168	0.321	1.489	-	1.193	98.00
0.5	21.23%	0.356	1.121	1.477	0.689		
2	45.76%	0.387	1.067	1.454	0.766		
4	20.00%	0.409	1.053	1.462	0.786		
5	21.12%	0.471	0.987	1.458	0.769		
10	23.16%	0.411	1.057	1.468	0.790		
15	24.31%	0.364	1.098	1.462	0.765		
20	26.09%	0.376	1.043	1.419	0.764		
30	30.12%	0.327	1.094	1.421	0.705		
45	35.37%	0.417	1.040	1.457	0.754		
60	40.20%	0.482	0.979	1.461	0.842	1.332	97.00

Table 206. Experiment 15 results. Matrix: MBR and light source: LED.

Time (minutes)	Degradation %	Absorbance					COD (ppm)
		Fe (II)	Fe (III)	Total iron	Hydrogen peroxide	UV-254	
0	0.00%	1.406	0.113	1.519	-	1.093	89.81
0.5	2.64%	0.381	0.118	0.499	0.742		
2	5.53%	0.399	1.090	1.489	0.753		
4	7.30%	0.400	1.094	1.494	0.749		
5	9.26%	0.381	1.135	1.516	0.756		
10	14.92%	0.301	1.170	1.471	0.740		
15	17.16%	0.367	1.156	1.523	0.740		
20	22.60%	0.384	1.097	1.481	0.737		
30	31.06%	0.418	1.100	1.518	0.729		
45	41.60%	0.556	0.951	1.507	0.727		
60	51.81%	1.406	0.113	1.519		1.491	72.19

Table 217. Experiment 16 results. Matrix: AEN and light source: LED.

Time (minutes)	Degradation %	Absorbance					COD (ppm)
		Fe (II)	Fe (III)	Total iron	Hydrogen peroxide	UV-254	
0	0.00%	1.545	0.000	1.537	-	0.968	96.00
0.5	29.49%	0.424	1,102	1.526	0.588		
2	32.39%	0.428	1,051	1.479	0.686		
4	45.73%	0.446	1,054	1.500	0.664		
5	35.75%	0.404	1,061	1.465	0.676		
10	37.19%	0.404	1,066	1.470	0.676		
15	39.13%	0.350	1,111	1.461	0.679		
20	40.74%	0.416	1,033	1.449	0.676		
30	44.72%	0.357	1,008	1.365	0.662		
45	51.43%	0.371	0,896	1.267	0.668		
60	55.18%	0.426	0,882	1.308	0.655	1.148	86.00